NUMERICAL SIMULATION OF TURBULENCE SUPPRESSION IN DEVELOPING TURBULENT PIPE FLOW DUE TO A RING DEVICE

Joseph C.S. Lai & Chongying Yang

Department of Aerospace & Mechanical Engineering
University College, The University of New South Wales
Australian Defence Force Academy, Canberra 2600, Australia.

ABSTRACT

The standard k-ε model and three low Reynolds number k-ε models were used to simulate developing turbulent pipe flow with a ring device installed in the near-wall region. While turbulence enhancement has been predicted by the standard k-ε model, the low Reynolds number models have predicted turbulence suppression up to 30 pipe diameters downstream of the device.

INTRODUCTION

Since the identification of coherent structures in a variety of fluid flows, considerable efforts have been devoted to controlling these structures using either active or passive means for practical applications. Large Eddy Break Up (LEBU) devices have been studied for drag reduction purposes. While there has been considerable debate as to whether a LEBU device produces net drag reduction, there is general consensus that a LEBU device does induce reduction in the skin friction drag in the flow being manipulated, although the drag introduced by such a device may more than offset such reduction. Since the purpose of a LEBU device is to break up the large eddies, it is usually located in the outer boundary layer. However, extensive turbulence measurements made by Hollis et al (1992) in fully-developed turbulent pipe flow indicate that turbulence has been suppressed by installing a ring device in the near-wall region at $y^+=112$ where dominant shear stress production occurs. This phenomenon of turbulence suppression has also been predicted by the numerical simulations of Lai & Yang (1995). Of the models used to predict turbulent flows, the most popular model is the two-equation k-ε model. The standard k-ε model developed by Launder & Spalding (1974) for high Reynolds number flows employs wall functions. Lam & Bremhorst(1981) and several other researchers have extended the original k-ε model to the low Reynolds number (Re) form which allows calculations right to the wall. In a systematic study, Patel et al(1985) found that the low Re k-ε models due to Lam & Bremhorst(1981) , Launder & Sharma(1974) and Chien(1982) and the model of Wilcox & Rubesin(1980) perform considerably better than others. These low Re k-ε models are essentially similar to that of Lam & Bremhorst(1981) except for the specific choice of the damping functions f_μ, f_1 and f_2. Owing to a lack of reliable experimental data, these near-wall modifications have largely been based on dimensional reasoning, intuition, and indirect testing. As pointed out by Rodi & Mansour(1993), even the more established models fail to reproduce the near-wall flow characteristics in detail. Thus, Rodi & Mansour deduced new forms of k-ε models based on direct numerical simulation (DNS) data. In an effort to overcome some of the deficiencies of k-ε models (such as arbitrary definition of near-wall pseudodissipation rate), a new time scale based k-ε model for near-wall turbulence was proposed by Yang and Shih(1993).

The objective of this study was to explore numerically the phenomenon of turbulence suppression in developing turbulent pipe flows at Re=240,00 with a ring device located at $y^+=112$. The standard k-ε model (LS) developed by Launder & Spalding(1974), the Lam & Bremhorst model(1981) (LB), the Rodi & Mansour model(1993)) (RM) and the Yang & Shih (1993) new time scale based k-ε model (YS) were used. The performance of each model in simulating this type of flow will be discussed. In particular, the ability of these models to predict the phenomenon of suppression of turbulence kinetic energy will be examined.

GOVERNING EQUATIONS AND BOUNDARY CONDITIONS

Consider a ring device installed in the fully-developed flow region in a pipe as shown in Fig.1. In cylindrical coordinates, the Reynolds' time-averaged momentum and continuity equations are given by equations (1) - (3). The effective viscosity μ_{eff} is given by $(\mu + \mu_t)$. For the four turbulence models used here, the turbulent viscosity μ_t is determined from $\mu_t = c_\mu f_\mu \rho k^2/\varepsilon$ with k and ε to be computed from the modelled transport equations (4) and (5) for k and ε respectively. While the constants c_1=1.45, c_2=1.90 and c_μ=0.09 are the same for the four turbulence models considered here, the other constants and functions for each model are summarized by Lai & Yang(1995).

$$\frac{\partial}{\partial x}(\rho uu) + \frac{1}{r}\frac{\partial}{\partial r}(\rho rvu) - \frac{\partial}{\partial x}(\mu_{eff}\frac{\partial u}{\partial x}) - \frac{1}{r}\frac{\partial}{\partial r}(r\mu_{eff}\frac{\partial u}{\partial r}) = S_u \quad (1) \qquad \frac{\partial}{\partial x}(\rho uv) + \frac{1}{r}\frac{\partial}{\partial r}(\rho rvv) - \frac{\partial}{\partial x}(\mu_{eff}\frac{\partial v}{\partial x}) - \frac{1}{r}\frac{\partial}{\partial r}(r\mu_{eff}\frac{\partial v}{\partial r}) = S_v \quad (2)$$

continuity: $$\frac{\partial(\rho u)}{\partial x} + \frac{1}{r}\frac{\partial(\rho rv)}{\partial r} = 0 \quad (3)$$

where $$S_u = \frac{\partial}{\partial x}(\mu_{eff}\frac{\partial u}{\partial x}) + \frac{1}{r}\frac{\partial}{\partial r}(r\mu_{eff}\frac{\partial v}{\partial x}) - \frac{\partial p}{\partial x} \qquad S_v = \frac{\partial}{\partial x}(\mu_{eff}\frac{\partial u}{\partial r}) + \frac{1}{r}\frac{\partial}{\partial r}(r\mu_{eff}\frac{\partial v}{\partial r}) - 2\mu_{eff}\frac{v}{r^2} - \frac{\partial p}{\partial r}$$

k: $$\frac{\partial}{\partial x}(\rho uk) + \frac{1}{r}\frac{\partial}{\partial r}(\rho rvk) - \frac{\partial}{\partial x}[(\mu + \frac{\mu_t}{\sigma_k})\frac{\partial k}{\partial x}] - \frac{1}{r}\frac{\partial}{\partial r}[r(\mu + \frac{\mu_t}{\sigma_k})\frac{\partial k}{\partial r}] = G_k - \rho\varepsilon \quad (4)$$

ε: $$\frac{\partial}{\partial x}(\rho u\varepsilon) + \frac{1}{r}\frac{\partial}{\partial r}(\rho rv\varepsilon) - \frac{\partial}{\partial x}[(\mu + \frac{\mu_t}{\sigma_\varepsilon})\frac{\partial \varepsilon}{\partial x}] - \frac{1}{r}\frac{\partial}{\partial r}[r(\mu + \frac{\mu_t}{\sigma_\varepsilon})\frac{\partial \varepsilon}{\partial r}] = (c_1 f_1 G_k - c_2 f_2 \rho\varepsilon)/T + E \quad (5)$$

where $$G_k = \mu_{eff}\{ 2[(\frac{\partial u}{\partial x})^2 + (\frac{\partial v}{\partial r})^2 + (\frac{v}{r})^2] + (\frac{\partial u}{\partial r} + \frac{\partial v}{\partial x})^2 \}$$

The inlet conditions are uniform velocity profile with the inlet kinetic energy and dissipation rate being given by $0.005U_b^2$ and $c_\mu k^{3/2}/(0.03R)$ respectively. At the outlet boundary, the flow is assumed to be fully-developed and v is set to zero. Zero gradient boundary conditions are applied at the axis of symmetry where the transverse velocity component v must also vanish. For the LB, RM and YS models, the physical boundary conditions for k and ε are directly implemented, i.e., $k_{wall} = 0$ with ε_{wall} being listed in Table 1 of Lai & Yang(1995).

RESULTS

The conservation and modelled transport equations were discretised and solved using the SIMPLE (Semi-Implicit for Pressure-Linked Equations) algorithm described by Patankar(1980). The computational domain covers $0 \le r/R \le 0.5$ and $0 \le x/D \le 60$. Nonuniform grids were used , with 99x27 grid points for the LS model and 143x87 grid points for the LB, RM and YS models. The computer codes were first validated by computing fully-developed turbulent pipe flows without a ring device. All the calculations reported were performed on a SUN SPARC 1000 workstation for pipe flow Reynolds number Re=240,000 with a ring device of length 10mm and thickness 0.635 mm installed at y^+=112(2.84 mm).

Velocity Distributions

Fig. 2 displays the radial distributions of normalised velocity differences $(u_d-u_{nd})/U_b$ for x^+=0, 500 and 3000. Here u_d and u_{nd} are the mean axial velocities with and without a ring device respectively. The wake of the ring device can be readily identified at x^+=0 and by x^+=3000, the velocity distributions have recovered to within 10% of the corresponding flow without the ring device. The agreement between the four models is good with the results of the RM model yielding the most departure from those of the other three models.

Turbulence Kinetic Energy Distributions and Turbulence Suppression

The radial distributions of turbulence kinetic energy for x^+=0 and x^+=3000 are shown in Figs. 3(a) and (b) respectively. The turbulence kinetic energy at x^+=0 is very high and has exceeded the values near the wall measured by Laufer(1954) for fully-developed pipe flow. By x^+=3000, however, the turbulence kinetic energy has been reduced significantly, particularly near the wall. Contours of dimensionless turbulence kinetic energy, defined as $(k_d - k_{nd})/u_\tau^2$, shown in Fig. 4 indicate increase in turbulence kinetic energy in the immediate neighbourhood of the ring device for all 4 models although they differ in details. Here k_d and k_{nd} are the turbulence kinetic energy with and without the ring device respectively. While the low Re models all predict turbulence suppression everywhere for 10D downstream, the LS model actually predicts turbulence enhancement. By integrating the contours in Fig.4 in the transverse direction, the suppression of turbulence kinetic energy can be expressed as $(K_d - K_{nd})/K_{nd}$. As shown in Fig.5., all three low Re models predict turbulence suppression up to x/D=30 with maximum suppression of almost 60% predicted by the YS model. On the other hand, the standard LS model predicts only increase in turbulence energy for all x/D. All four models predict as much as 50% skin friction reduction within x/D=1 (Fig.6).

CONCLUSIONS

The phenomenon of turbulence suppression in developing turbulent pipe flow due to a ring device has been predicted by all three low Re models. However, they differ in predicting the magnitude of turbulence suppression with a maximum suppression of almost 60%, 40% and 20% for the YS, RM and LB models respectively. On the other hand, only increase in turbulence kinetic energy has been predicted by the standard k-ε (LS) model.

ACKNOWLEDGEMENT

This project has been supported by the Australian Research Council.

REFERENCES

Chien K.Y., 1982 "Predictions of channel and boundary-layer flows with a low-Reynolds-number turbulence model", *AIAA Journal* **20**, pp. 33-38.

Hollis, P. G., Lai, J.C.S. & Bullock, K.J., 1992 "What happens if a LEBU device is inserted in the near wall region", *Proceedings 11th Australasian Fluid Mech Conf.*, Hobart, Australia, pp. 547-550.

Lai, J.C.S. & Yang, C., 1995 "Numerical simulation of turbulence suppression in fully-developed pipe flow due to a ring device", *Proceedings First Asian CFD Conf.*, pp. 549-554.

Laufer, J., 1952 "The structure of turbulence in fully developed pipe flow", NACA 1174.

Lam, C.K.G. & Bremhorst, K.,1981 "A modified form of the k-ε model for predicting wall turbulence",*ASME J. Fluids Engng.* **103**, pp. 456-460.

Launder, B. E. & Sharma, B. I., 1974 " Application of the energy-dissipation model of turbulence to calculation of flow near a spinning disc", *Letters in Heat and Mass Transfer* **1**, pp.131-138.

Launder, B.E. & Spalding, D.B., 1974 "The numerical computation of turbulent flows", *Comp. Meth. Appl. Mech. Engng.* **3**, pp.269-298.

Patankar, S.V., 1980 " Numerical Heat Transfer and Fluid Flow ", McGraw Hill, NY.

Patel, V.C., Rodi, W. & Scheuerer, G., 1985 " Evaluation of turbulence models for near-wall and low-Reynolds number flows", *AIAA Journal* **23**, pp.1308-1319.

Pun, W. M. and Spalding, D. B.,1976 "A General Computer Program for Two-Dimensional Elliptic Flows",HTS/76/2, Imperial College.

Rodi W. & Mansour N. N., 1993 " Low Reynolds number k-ε modelling with the aid of direct simulation data",*J. Fluid Mech.* **250**, pp.509-529.

Wilcox, D. C. and Rubesin, W. M.,1980 " Progress in turbulence modeling for complex flow fields including effects of compressibility", NASA Tech. Paper 1517.

Yang Z. & Shih T. H.,1993 "New time scale based k-ε model for near-wall turbulence", *AIAA Journal*, **31**, pp.1191-1198.

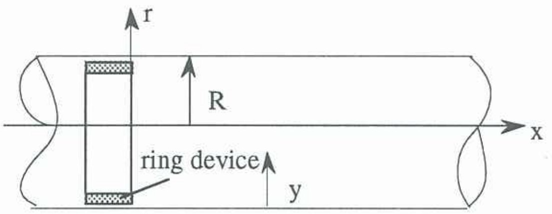

FIG.1 SCHEMATIC DIAGRAM OF FLOW GEOMETRY.

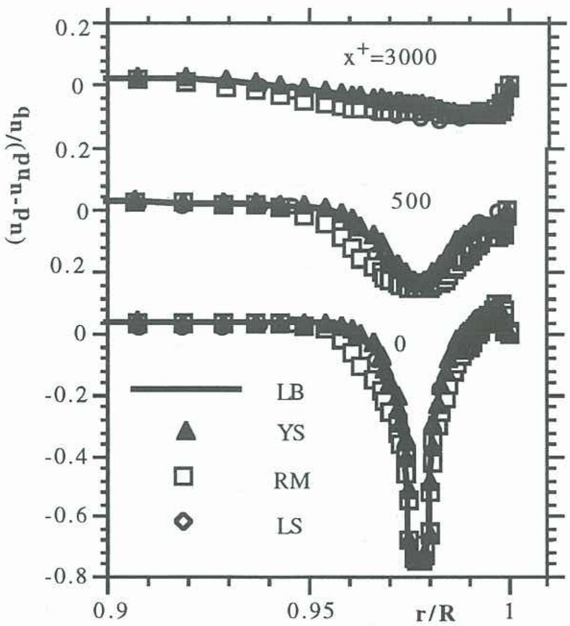

FIG.2 VARIATION OF NORMALISED VELOCITY DIFFERENCES WITH r/R.

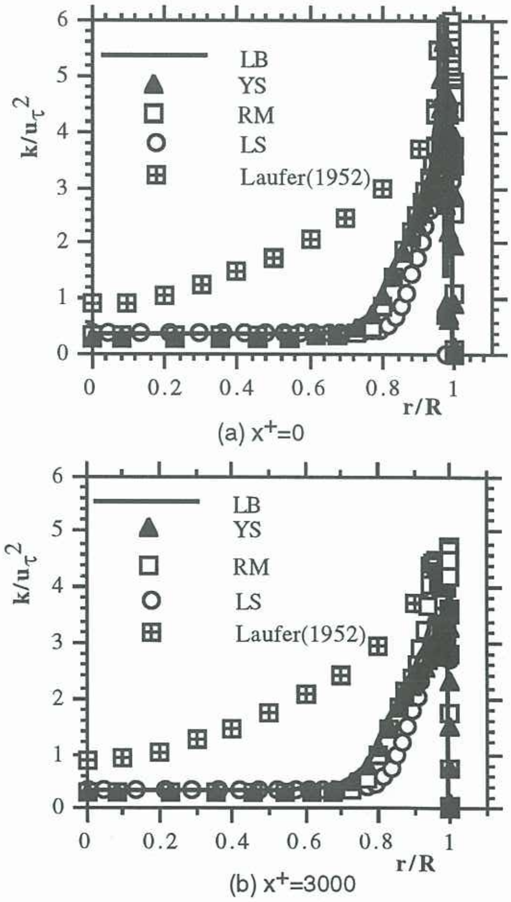

FIG.3 DISTRIBUTION OF TURBULENCE KINETIC ENERGY

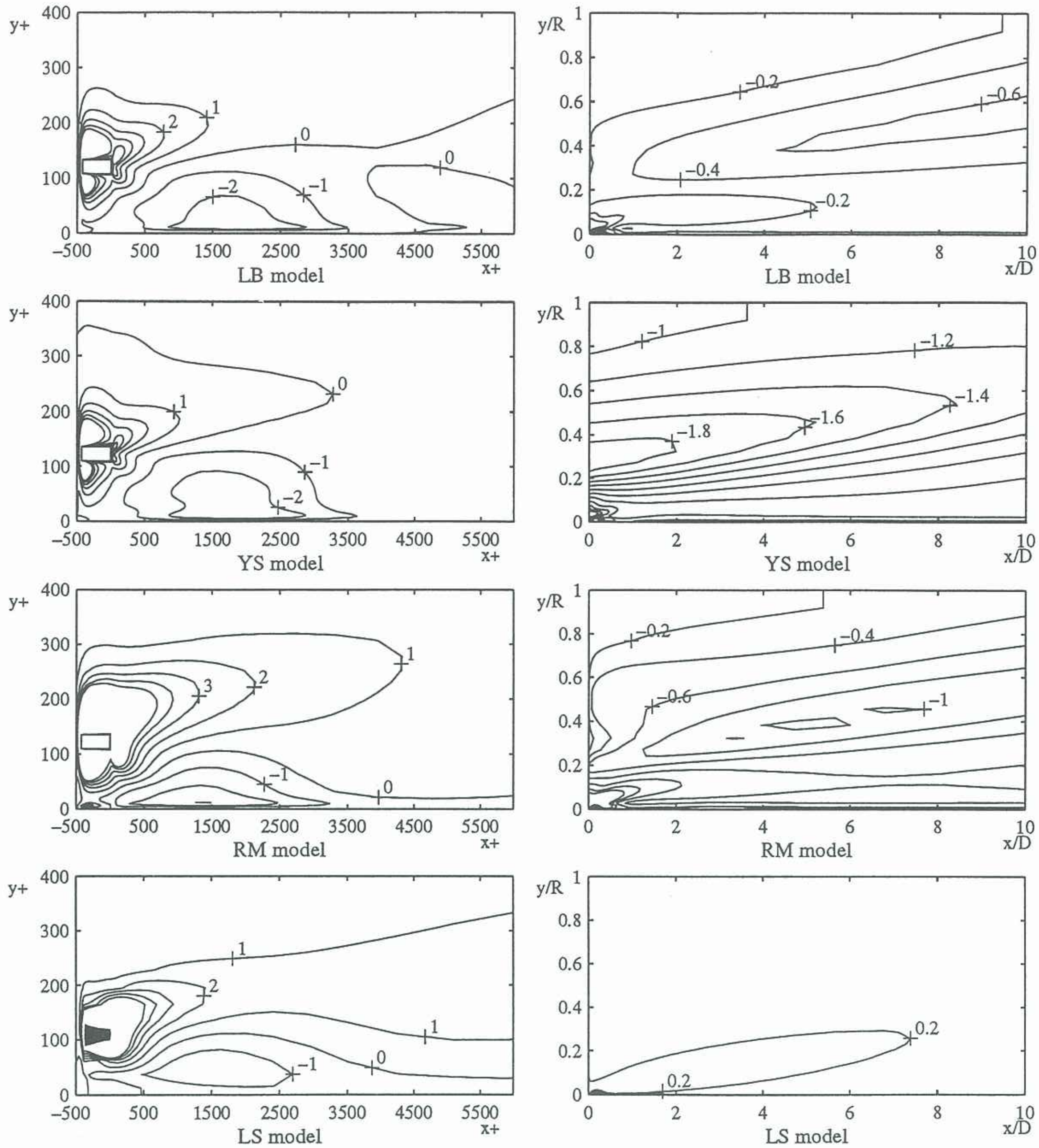

FIG. 4 CONTOURS OF DIMENSIONLESS TURBULENCE KINETIC ENERGY DIFFERENCE $(k_d-k_{nd})/u_\tau^2$ BETWEEN FLOWS WITH AND WITHOUT A RING DEVICE.

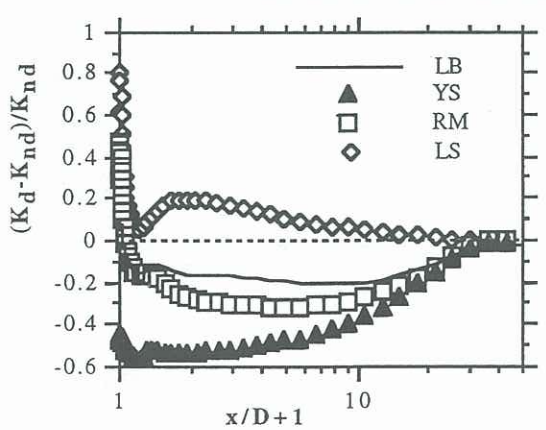

FIG. 5 VARIATION OF SUPPRESSION OF TURBULENCE KINETIC ENERGY WITH AXIAL DISTANCE.

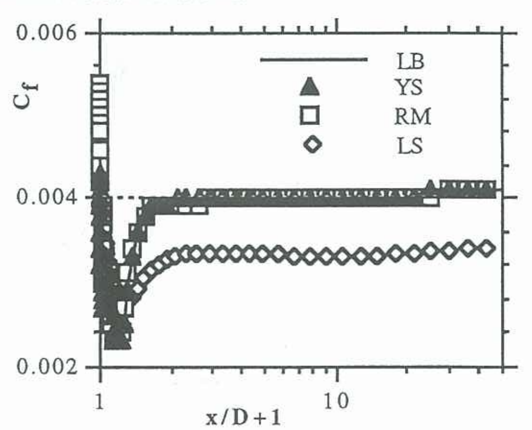

FIG. 6 VARIATION OF SKIN FRICTION COEFFICIENT WITH AXIAL DISTANCE.